Xanthophylls in Light-Harvesting Complex II of Higher Plants: Light Harvesting and Triplet Quenching[†]

Erwin J. G. Peterman,* Claudiu C. Gradinaru, Florentine Calkoen, Jeroen C. Borst, Rienk van Grondelle, and Herbert van Amerongen

Department of Physics and Astronomy and Institute for Molecular Biological Sciences, Vrije Universiteit, De Boelelaan 1081, 1081 HV Amsterdam, The Netherlands

Received May 19, 1997; Revised Manuscript Received July 21, 1997[⊗]

ABSTRACT: A spectral and functional assignment of the xanthophylls in monomeric and trimeric light-harvesting complex II of green plants has been obtained using HPLC analysis of the pigment composition, laser-flash induced triplet-minus-singlet, fluorescence excitation, and absorption spectra. It is shown that violaxanthin is not present in monomeric preparations, that it has most likely a red-most absorption maximum at 510 nm in the trimeric complex, and that it is involved in both light-harvesting and Chl-triplet quenching. Two xanthophylls (per monomer) have an absorption maximum at 494 nm. These play a major role in both singlet and triplet transfer. These two are most probably the two xanthophylls resolved in the crystal structure, tentatively assigned to lutein, that are close to several chlorophyll molecules [Kühlbrandt, W., Wang, N. D., & Fujiyoshi, Y. (1994) *Nature 367*, 614−621]. A last xanthophyll contribution, with an absorption maximum at 486 nm, does not seem to play a significant role in light-harvesting or in Chl-triplet quenching. On the basis of the assumption that the two structurally resolved xanthophylls are lutein, this 486 nm absorbing xanthophyll should be neoxanthin. The measurements demonstrate that violaxanthin is connected to at least one chlorophyll *a* with an absorption maximum near 670 nm, whereas the xanthophylls absorbing at 494 nm are connected to at least one chlorophyll *a* with a peak near 675 nm.

In photosynthesis, the harvesting of solar photons by the antenna pigments is of great importance for the efficiency of the photosynthetic process (*1*). Light-harvesting complex II (LHCII) is the most abundant light-harvesting antenna pigment-protein complex in plants. It binds about half of the chlorophylls (Chl's)[1] present in the chloroplast. The complex is normally isolated as a trimer, which is also believed to be the natural form. Chemical (HPLC) analyses have shown that each monomer binds five or six Chl *b*, seven or eight Chl *a*, and several xanthophyll (Xan) molecules: two luteins (Lut), one neoxanthin (Neo), and varying, substoichiometric amounts of violaxanthin (Vio) (one-half to one) (*2*). The Xan's serve several functions in LHCII. First of all they protect the plant against singlet oxygen which can be formed by excitation transfer from Chl triplet states to (ground state) triplet oxygen (*3*). Recently, we have shown (*4*) that in LHCII the Chl triplet states are totally quenched by the Xan's (at room temperature), thus shortening the lifetime of the Chl triplet states several orders of magnitude. A second function of the Xan's in LHCII is light-harvesting of blue/green light. It has been shown that Xan's transfer efficiently (∼100%) (*5*) their excitations to Chl *a*, the species with the singlet excited state lowest in energy in LHCII. A third function of the Xan's in LHCII is stabilization of the complex. No stable complexes can be formed in reconstitution experiments in the absence of Xan's (*6*, *7*). The importance of the Xan's in stabilizing the complex is also clear from the crystal structure, which indicates that two Xan's in the center of the complex might be hydrogen-bonded with both sides to different parts of the protein, seemingly forming an internal crossbrace (*8*).

The structural model at 3.4 Å resolution, obtained with the use of electron microscopy and electron diffraction of two-dimensional crystals, only shows two Xan's in the center of the complex, the others are not resolved. These molecules were assigned to Lut's. The structural model shows the short distances between the Xan's and Chl's (for the Chl's closest to the two Lut's about 4 Å), which are required for efficient triplet and singlet energy transfer between the species (*9*). The resolution of the model was not high enough to distinguish between Chl *a* and *b*. A tentative assignment of the Chl's was based on the proximity of 7 Chl's to the two central Lut's. It was argued that triplets only will be formed on the Chl *a* molecules, because the energy transfer from Chl *b* to *a* is much faster than the formation of triplets (picosecond vs nanosecond). This implies that only Chl *a* triplets need to be quenched, suggesting that the Chl *a*'s are closest to the Xan's. This assignment holds the assumption that only the two structurally resolved Xan's are involved in the triplet-quenching mechanism. This is not in agreement with studies of the triplets in LHCII (*10*−*12*, *4*), which all suggest that more Xan's are involved. All these studies revealed at least two spectrally distinct Xan contributions to the triplet-minus-singlet absorption (T−S) spectra, which

[†] This work was supported by the Netherlands Foundation for Scientific Research (NWO) via the Foundation for Life Sciences (SLW) and the European Union, Grant CT 940619.

* Corresponding author. Tel: +31 20 444 7941. Fax: +31 20 444 7899. E-mail: erwinp@nat.vu.nl.

[⊗] Abstract published in *Advance ACS Abstracts,* September 15, 1997.

[1] Abbreviations: 1-T, 1 - transmission spectrum; Chl, chlorophyll; DM, *n*-dodecyl β-D-maltoside; Lut, lutein; Neo, neoxanthin; plA_2, phospholipase A_2; T−S, triplet-minus-singlet absorption; Xan, xanthophyll; Vio, violaxanthin; w/v, weight per volume; w/w, weight per weight.

S0006-2960(97)01168-9 CCC: $14.00

peak at 525 and 506 nm. These spectra seem to be associated with bands in the absorption spectrum at 510 and 494 nm respectively (*4*). Under aerobic conditions at room temperature the two Xan triplets could also be discriminated by their lifetimes, due to a difference in the efficiency of triplet quenching by oxygen. It has been attempted to assign the T−S signals to the Xan species (*10*, *12*), but the results were not conclusive.

The efficiency of the triplet transfer from Chl to Xan has been estimated to decrease from 100% at room temperature to 82% at 4 K (*4*). An interesting aspect of the Xan triplets is that they also give rise to pronounced absorption changes in the Chl *a* Q_y region (660−690 nm) (*10*, *4*). The precise origin of these signals is unclear, but they clearly demonstrate the close contacts between Xan and Chl *a* molecules.

Recently, two reports have appeared on ultrafast Xan-to-Chl singlet energy transfer in LHCII (*13*, *14*). The conclusion of both reports is quite contradictory. We interpret our ultrafast transient absorption kinetics of LHCII at 77 K (*13*) in terms of direct energy transfer from Xan-to-Chl *a* in 220 fs. Upon excitation of the Xan's at 500 or 514 nm we observed a considerable (∼25%) amount of instantaneous Chl *b* bleaching, which we interpret as direct excitation of Chl *b*. We also observed population of a Chl *a* pool absorbing more to the blue (∼670 nm) upon excitation of "red" absorbing Xan (excitation at 514 nm) and population of a Chl *a* pool absorbing more to the red (∼675 nm) upon excitation of "blue" absorbing Xan (excitation at 500 nm). This connection between red (blue) Chl *a* and blue (red) Xan, was also observed in ADMR experiments (*10*). Our interpretation of the ultrafast transient absorption kinetics is in sharp contrast to similar measurements at room temperature by Connelly and co-workers (*14*). They claim to observe no direct Chl *b* excitation (at 490 nm) and interpret their kinetics as 140 fs energy transfer from Xan to Chl *b*, followed by transfer from Chl *b* to Chl *a*.

In this contribution we present determination of the pigment contents and T−S and fluorescence excitation measurements for trimeric and monomeric LHCII, which enable us to spectrally assign the Xan's in LHCII. Part of the data has been presented in a preliminary form before (*15*).

MATERIALS AND METHODS

Sample Preparation

Trimeric LHCII was prepared and purified using the method described earlier (*4*), starting from BBY membrane fragments (*16*) from spinach, based on anion-exchange chromatography and using the detergent *n*-dodecyl *β*-D-maltoside (DM) for solubilization of the complexes. This preparation of the trimeric, major LHCII is essentially free of monomeric, minor LHCIIs (CP29, CP26), as checked with gel electrophoresis. LHCII monomers were obtained from trimers by incubation with phospholipase A_2 (plA_2, Sigma; 10 μg/mL) (*17*). The monomers were separated from free pigments and some remaining trimers using sucrose gradient (5−20% w/v) centrifugation (overnight at 200000*g*). For absorption and HPLC measurements the monomers were subjected to an extra purification step on an anion-exchange column, to get rid of all unbound pigments. For the low-temperature measurements LHCII was diluted in a buffer containing 20 mM Hepes (pH 7.5), 0.06% (w/v) DM, and 70% (v/v) glycerol. The temperature of the sample was regulated using a helium bath cryostat (Utreks) for the fluorescence measurements or a helium flow cryostat (Oxford Instruments) for the absorption and T−S measurements.

Pigment Analysis

The pigment composition of trimeric and monomeric LHCII was determined using HPLC. The LHCII samples were extracted on a C_{18} extraction column with methanol and loaded on a C_{18} Spherisorb reverse phase HPLC column. As liquid phase the first 15 min a mixture of acetonitrile (170 mL), methanol (27 mL), and 0.2 M Tris, pH 8, in water (3 mL) was applied, followed by a gradient (in 3 min) to 100% methanol. The HPLC system was equipped with a diode-array optical absorption detector, which allowed identification of the peaks in the chromatograms by their absorption spectra. To calculate the amount of pigments the extinction coefficients as published by Davies (*18*) and Lichtentaler (*19*) were used.

Spectroscopy

Absorption spectra were recorded on a Cary 219 spectrophotometer using an optical bandwidth of 0.5 nm. Fluorescence excitation spectra were measured on a home-built fluorometer. Modulated excitation light was provided by a tungsten-halogen lamp via a $^1/_2$-meter monochromator (Chromex 500SM, spectral bandwidth 1 nm) and a mechanical chopper. Fluorescence was detected in a 90° geometry, via a high-pass (>650 nm) filter by an S-20 photomultiplier and fed into a lock-in amplifier. At the same time the transmission of the sample was measured using a photodiode. The setup was calibrated for the wavelength dependence of the intensity of the excitation light using three different dyes (Styryl 9M, DCM, and LD722, all in methanol).

Microsecond laser-flash induced T−S absorption difference measurements were performed as described before (*4*). In short, excitation light was provided by a Nd:YAG (second harmonic) pumped dye laser. The excitation pulses had an intensity of ∼10 mJ, wavelength 590 nm (dye: Rhodamine 610) or 670−685 nm (dye: Pyridine 698). Detection light from a pulsed xenon lamp was detected continuously during the pulse via a $^1/_4$-m monochromator (bandwidth 2 nm) by a photomultiplier, connected to a digital oscilloscope. The response time of the setup was less than 0.5 μs. Time traces (averages of 8−64 shots) were detected at different wavelengths and analysed globally (*20*). The triplet transfer efficiency was calculated using for the Chl *a* triplets the extinction coefficient of the Chl *a* Q_y transition (1.0×10^5 M^{-1} cm^{-1}) and for the Xan triplets the extinction coefficient of the $T_n \leftarrow T_0$ transition of *β*-carotene (2.4×10^5 M^{-1} cm^{-1}) (*21*, *4*).

RESULTS

HPLC Pigment Analysis

The pigment composition of LHCII trimers and monomers is shown in Table 1. We did not determine the pigment to protein ratio. For better comparison of the relative abundance of the different pigments, we assumed six Chl *b* to be present per monomer, both for monomers and trimers. The amounts of the other pigments were scaled to this six Chl *b*

Table 1: Pigment Stoichiometry (Pigment Molecules per Monomer) in Monomeric and Trimeric LHCII As Determined with HPLC[a]

	trimeric LHCII	*monomeric* LHCII
lutein	1.82 ± 0.20	1.79 ± 0.14
neoxanthin	0.91 ± 0.16	0.76 ± 0.13
violaxanthin	0.21 ± 0.03	0.07 ± 0.02
chlorophyll *a*	8.28 ± 0.30	6.84 ± 0.24
chlorophyll *b*	6[b]	6[b]

[a] The values are averages ± standard errors of five independent experiments. [b] The amount of chlorophyll *b* was set to 6 per monomer, and the other pigments were scaled to this.

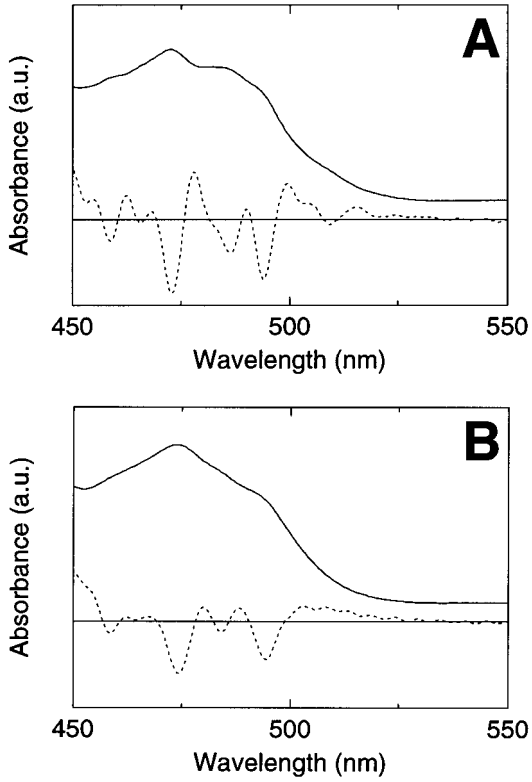

FIGURE 1: Absorption spectra (solid) and second derivatives (dotted) of trimeric (A) and monomeric (B) LHCII at 4 K in the region where the Xan's absorb.

per monomer. This is the amount of Chl *b* generally found for LHCII (*2*). The values obtained for trimers are very similar to those obtained before (*2*; *22*). Assuming the presence of two luteins per LHCII monomer these results indicate that LHCII contains more pigments (one Chl *a*, one Chl *b*, one Neo, and some Vio) than resolved in the structural model (*8*). The amount of Vio is substoichiometric. It is unclear whether this means that only part of the Vio binding sites are occupied or that only one Vio binding site per trimer is present or that some Vio is lost upon isolation, but it clearly indicates that our preparation is heterogeneous with respect to Vio. Upon plA$_2$-induced monomerization some Chl *a* is lost, in line with observations for similar preparations from pea (*17*). Furthermore, a significant fraction of Vio is lost.

Absorption Spectra

In Figure 1 the 4 K absorption spectra of monomeric and trimeric LHCII are shown. In general the spectrum of monomers is slightly less structured than that of trimers. Clear differences can be observed between trimers and monomers in the Car S_2 region. In the spectrum of trimers (Figure 1A) three shoulders (negative peaks in the second derivative) are present due to the red-most $S_2 \leftarrow S_0$ transition of the Xan's, at 510, 494, and 486 nm (*4*). The separation between these three shoulders is 635 and 333 cm^{-1}, respectively. The $S_2 \leftarrow S_0$ absorption spectra of carotenoids generally show a progression of a dominant C═C stretching mode, with a separation of about 1400−1500 cm^{-1} (*23*). Such a separation of vibronic bands strongly suggests that the three shoulders in the LHCII absorption spectrum mentioned above are due to spectrally distinct Xan molecules. In monomers only two of these shoulders can be observed, the one at 510 nm is missing. This is not only clear from the second derivative of the spectrum, also the absorption spectrum clearly shows a decrease of the absorption in the 510−520 nm region upon monomerization. A straightforward explanation for the disappearance of the 510 nm shoulder is the loss of a major fraction of the Vio upon monomerization, which would imply that the 510 nm peak in the absorption spectrum of trimers is due to Vio. Furthermore, the 510 nm band is not very intense. The intensity of this band corresponds to a substoichiometric amount of Xan (see below). If the 510 nm band would be due to either Neo or Lut it should be much more intense.

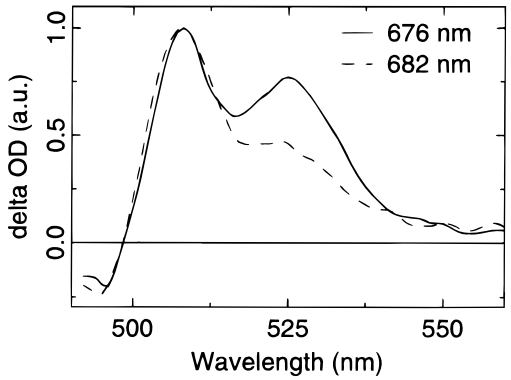

FIGURE 2: T−S spectra of LHCII trimers at 4 K upon excitation at 676 nm (solid line) and 682 nm (dashed line). The spectra are the decay-associated spectra obtained from global analysis (1 spectrum, 2 decay times ∼8 and ∼50 μs due to decay from different ^{3}Xan spin sublevels) of each dataset consisting of time traces measured at different wavelengths. The spectra are normalized to one in the maximum.

Site-Selected T−S Spectra of LHCII Trimers

Using ADMR Van der Vos and co-workers observed (*10*) that in LHCII trimers red (blue) Xan is connected to blue (red) Chl *a*. Recently, in a study of the subpicosecond singlet energy transfer from Xan to Chl (*13*) we obtained results with the conclusion that excitation of Xan at 500 nm leads to fast population of red (∼675 nm) Chl *a*, while excitation at 514 nm gives a fast population of blue (∼670 nm) Chl *a*. We investigated whether we could also observe this specific Xan−Chl *a* contact in our T−S spectra of LHCII trimers upon selective excitation in the Chl *a* pool. The 4 K T−S spectra obtained upon excitation at 676 and 682 nm are shown in Figure 2. It is clear that upon selective excitation in the Chl *a* region the ratio between the two triplet contributions (peaking at 506 and 525 nm) is altered: excitation in the extreme red (682 nm) leads to a relative decrease of the 525 nm peak, excitation more to the blue to an increase of this peak. These results again indicate specific connections between "red" absorbing Chl *a* and "blue" Xan [peaking in the T−S spectrum at 506 nm and in the

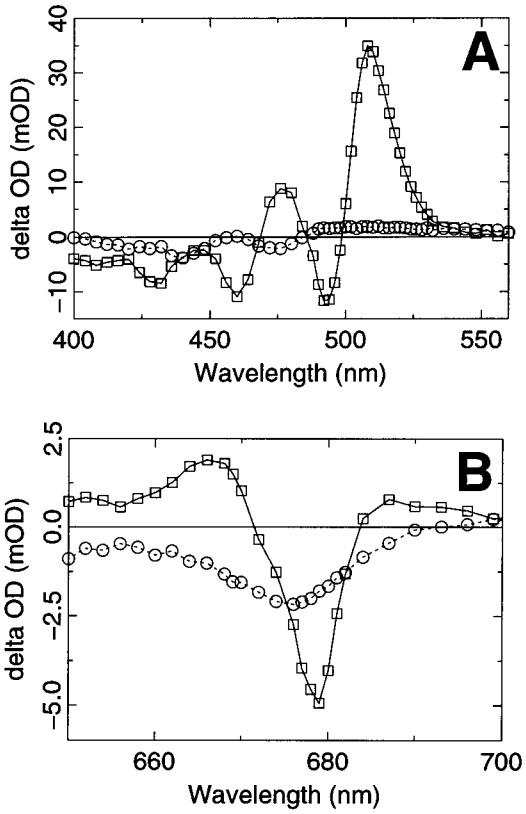

FIGURE 3: T−S spectra of LHCII monomers at 77 K. The spectra are the decay associated spectra of the two components obtained from global analysis of a dataset consisting of time traces measured at different wavelengths. Solid line, the 12 μs (^{3}Xan) component; dotted line, the ∼ms (^{3}Chl *a*) component. In A the Xan S_2 and Chl Soret region are shown; in B the Chl *a* Q_y region is shown.

absorption spectrum at 494 nm (*4*)] and between "blue" absorbing Chl *a* and "red" Xan (T−S peak at 525 nm, due to absorption peak at 510 nm).

It is quite surprising that it is possible to populate different Xan triplets upon selective excitation. One might expect that whatever the excitation wavelength is, only the lowest Chl *a* singlet state would be populated on a picosecond time scale at low temperatures. However, inhomogeneous broadening plays an important role: the excited state energy of a specific pigment on a well-defined binding place can vary around a certain average value. This means that if a certain pigment has on the average a lower excited state energy than another one, there is still a probability that in some complexes the excited state energy of the former pigment is higher than that of the lattter pigment. This probability depends on the difference in average values of the energies and the width of the distributions. Many Chl's contribute to the absorption in the main low energy band of LHCII (around 676 nm) (*24*). It seems that the pigments that have on the average the lowest excited state energy are connected more to the Xan's with their T−S maxima at 506 nm. Another explanation of the effect of selective excitation might be heterogeneity of the sample. Some complexes might not contain the Xan with a T−S maximum at 525 nm. If these have a slightly red-shifted Q_y absorption the observed selectivity can be expected.

T−S Spectra of LHCII Monomers

In Figure 3 the T−S spectra of monomeric LHCII at 77 K are shown. The spectra show that apart from a major ^{3}Xan component also a ^{3}Chl *a* contribution is present. The ^{3}Xan in LHCII monomers decays to the ground state in 12 μs, very similar to what is observed for LHCII trimers (*4*). The spectrum however is quite different: it only shows the contribution of one Xan, peaking at 508 nm. The peak in the T−S spectrum of trimers at 525 nm (see Figure 2) is not present in the spectra of monomers. We have suggested before (*4*) that this latter contribution in the T−S spectrum is connected to the peak in the absorption spectrum at 510 nm. In monomers both the shoulder in the absorption spectrum at 510 nm (see Figure 1) and the peak in the T−S spectrum at 525 nm are missing, supporting this suggestion. It is clear from the bleaching at 494 nm in the T−S spectrum of monomers that the T−S maximum at 508 nm is due to the shoulder in the absorption spectrum at 494 nm.

Also for the monomers changes in the Chl *a* absorption region are observed with a lifetime of 12 μs. We attribute these signals to Xan−Chl interactions that are affected upon triplet formation on a Xan (*4*). The Xan T−S signal for monomers in the Chl *a* region is very similar to the signal measured for trimers at 77 K (bleaching at 678 nm, with a shoulder at 672 nm, small positive features at 653 and 667 nm). However the signal does not change upon lowering the temperature to 4 K (not shown), as is the case for trimers (*4*) for which a bleaching at 680 nm grows in.

Also shown in Figure 3 is the ^{3}Chl component, with a lifetime of ∼ms [too long to estimate more accurately because of the short time base used (100 μs)]. Contributions of Chl *a* (at 676 and 440 nm) and some Chl *b* (at ∼650 and 475 nm) are observed. To some extent these triplets might be due to unbound Chl's. However, the observed ^{3}Chl *a* minimum is at 676 nm, more to the red than expected for Chl *a* in detergent (*25*). Therefore, we conclude that the major fraction of the ^{3}Chl *a* is due to bound Chl *a*. We conclude that all ^{3}Chl *b* is due to unbound Chl *b*, because bound Chl *b* would transfer efficiently and fast singlet excitations to Chl *a*, before a Chl *b* triplet can be formed. We estimate the efficiency of the triplet transfer from Chl *a* to Xan in LHCII monomers at 77 K to be 80% ± 5%. This efficiency does not change upon lowering the temperature to 4 K (not shown). This is in contrast to LHCII trimers for which the efficiency decreases from 94% ± 2% at 77 K to 82% ± 7% at 4 K (*4*). It should be noted that we used *in vitro* values for the extinction coefficients to calculate these efficiencies and did not consider alterations of these coefficients due to the LHCII environment and temperature dependence.

Reconstruction of the 525 nm T−S Component of LHCII Trimers

To furthermore demonstrate that the contribution peaking at 525 nm is indeed due to a single Xan and to find a minimum in the T−S spectrum which might correspond to the singlet absorption maximum at 510 nm, we tried to reconstruct this T−S component. The results of three different reconstruction procedures are shown in Figure 4. The three methods [(a) the difference T−S spectrum of trimers and monomers; (b) the difference of the T−S spectra for trimers excited at 676 and 682 nm; (c) shift of the T−S spectrum of monomers] yield similar results. All three spectra show a peak at 525 nm [which was imposed for spectrum (c)] with a corresponding minimum near 511 nm.

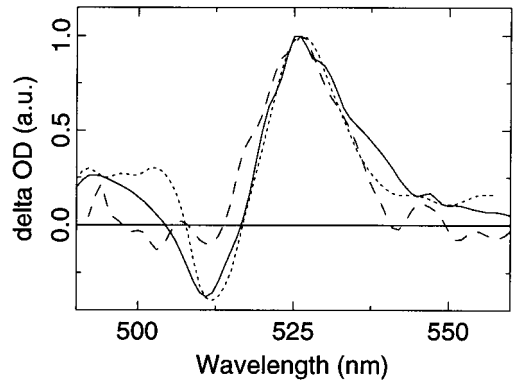

FIGURE 4: Reconstruction of the 525 nm component in the T−S spectrum of LHCII trimers using different methods. Solid line, the T−S spectrum of LHCII monomers shifted 17 nm to the red; dotted line, the difference between the T−S spectra of LHCII trimers minus monomers (the latter spectrum was shifted 1 nm to the blue, both spectra were normalized in the maximum); dashed line, the difference between the T−S spectra of LHCII trimers excited at 676 and 682 nm.

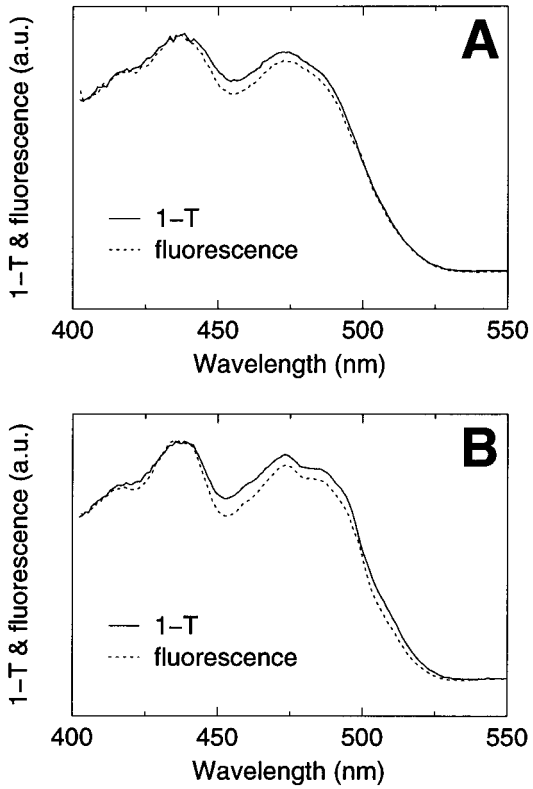

FIGURE 5: Fluorescence excitation spectra (dotted) compared to 1-minus-transmission spectra (solid) of LHCII trimers at 300 (A) and 40 K (B). The spectral bandwidth was in both cases 1 nm. The fluorescence was detected via a high-pass filter (>650 nm). Both spectra are normalized in their maxima.

The minimum at 511 nm supports the connection we proposed (*4*; see above) between the 525 nm component in the T−S spectrum and the shoulder in the absorption spectrum of trimers at 510 nm. Method a furthermore shows that in trimers the contributions at 525 has an intensity which is about 45% ± 5% of that at 506 nm.

Fluorescence Excitation Spectra of LHCII Trimers

In Figure 5 a comparison is shown between the excitation and 1-minus-transmission (1−T) spectra of LHCII trimers at 300 and 40 K. In bacteriochlorophyll-binding complexes

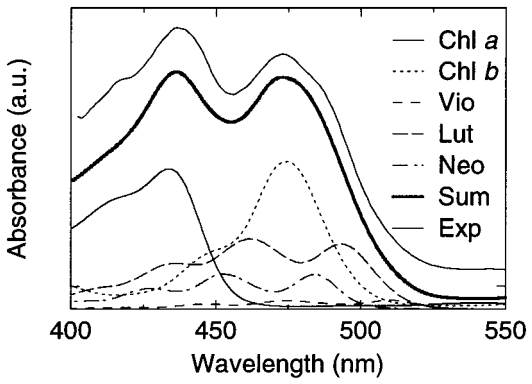

FIGURE 6: Experimental absorption spectrum of LHCII (room temperature, solid line, with offset) together with reconstructed spectrum (fat, solid line) from the five pigments present in the complex: Chl *a* (solid), Chl *b* (dotted), Vio (short dashes), Lut (long dashes), and Neo (solid dash). For details see text.

(*9*), the bacteriochlorophyll Q_x transition can be used as an internal standard to scale excitation and 1−T spectra. For LHCII such a scaling is not possible due to the absence of a clear Chl Q_x transition near the region of interest (400−560 nm) and a strong overlap of Xan and Chl Soret bands. The spectra in Figure 5 are normalized at their maxima; only shapes can be compared directly (see below). At 300 K, excitation and 1−T spectra show only a slight difference from about 440 to 490 nm. At 40 K the difference is more pronounced, again from about 440 to 490 nm but also between 500 and 520 nm.

To get a more quantitative insight in the efficiency of Xan-to-Chl excitation transfer we have attempted to reconstruct the LHCII absorption spectrum in the 400 to 550 nm region using spectra of the five isolated pigments (Chl's in acetone, Xan's in 3-methylpentane). The result is shown in Figure 6. To obtain this reconstruction we have shifted the pigment spectra to the wavelengths where they are concluded to be, on the basis of the absorption (Figure 1) and T−S spectra (*4*): Chl *a* at 435 nm, Chl *b* at 475 nm, and the red-most peaks of the Xan's at 486, 494, and 510 nm (see below). For the extinction coefficients a ratio of 0.5:0.7:1 for Chl *a*:Chl *b*:Xan's was used (for the Chl's the values in methanol for the Xan's those in hexane were taken) (*18*, *19*). For the pigment stoichiometry a ratio of 8:6:2:1:0.25 for Chl *a*:Chl *b*:Lut:Neo:Vio (Table 1) was used. A reasonable reconstruction of the absorption spectrum could only be obtained when the substoichiometric amount of Vio was positioned at 510 nm. Putting either Lut or Neo there would lead to too much absorption around 510 nm. A slightly better description of the absorption spectrum was obtained when two Xan's are put at 494 nm and one at 486 nm, instead of the other way around. Assuming that both Lut molecules absorb at the same wavelength, the Lut's are shifted to 494 nm. Consequently, the single Neo molecule has a peak at 486 nm (a more thorough discussion of the Xan assignments will be given in the Discussion). It should be noted that the spectra of the Xan's partially overlap. However, the separation of the spectral features is such, that this does not hinder a clear spectral distinction, as can be seen from the simulations below. In the rest of this paragraph we will denote the different spectral Xan contributions with their red most absorption maximum (510, 494, and 486 nm). The result of the reconstruction using these assumptions is shown in Figure 6. We want to stress that our reconstructed

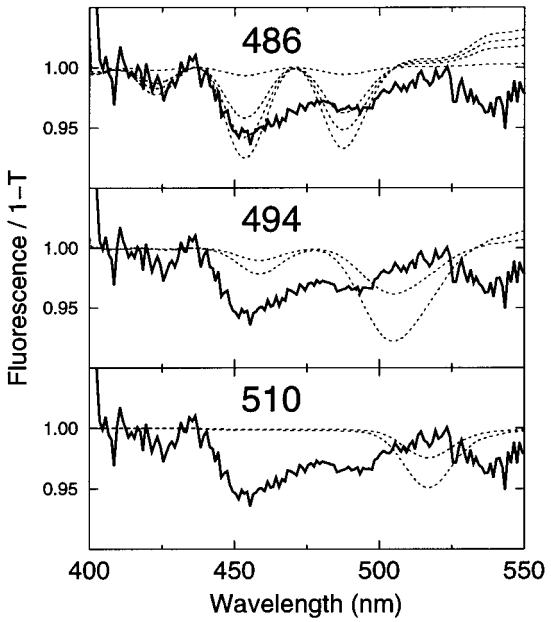

FIGURE 7: Comparison of the experimental (solid line) and simulated (dashed) ratio of fluorescence excitation and 1−T spectra at 300 K. The simulated spectra were calculated using the reconstructed absorption spectrum (Figure 6). For the 486 nm Xan ratio's are shown for 90%, 40%, 20%, and 0% Xan-to-Chl transfer efficiency (from top to bottom); for the 494 nm Xan for 90% and 80% efficiency; for the 510 nm Xan for 90% and 80% efficiency. For details see text.

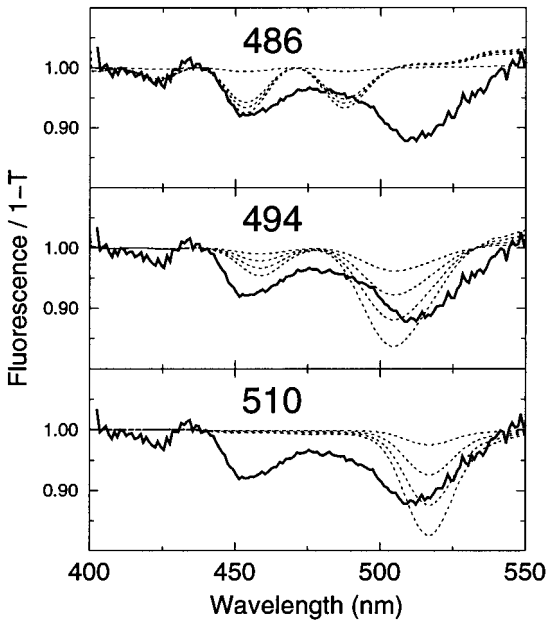

FIGURE 8: Comparison of the experimental (solid line) and simulated (dashed) ratio of fluorescence excitation and 1−T spectra at 40 K. Note the different *y*-scaling compared to figure 7. The simulated spectra were calculated using the reconstructed absorption spectrum (Figure 6). For the 486 nm Xan ratio's are shown for 90%, 20%, 10%, and 0% Xan-to-Chl transfer efficiency (from top to bottom); for the 494 nm Xan for 90%, 80%, 70%, and 60% efficiency; for the 510 nm Xan for 90%, 70%, 50%, and 30% efficiency. For details see text.

spectrum is supposed to be a reasonable, straightforward description of the absorption spectrum for simulating the fluorescence excitation spectra; it is certainly not a fit or an attempt to describe all details of the absorption spectrum at different temperatures. For this we lack too many parameters like bandwidths and extinction coefficients of the pigments in the protein. We checked whether changes in bandwidths and extinction coefficients changed the outcome of the simulations of the excitation spectra significantly, but the effects are small. In our recent study of ultrafast Xan-to-Chl excitation transfer (*13*) we have used the reconstructed spectrum to estimate the selectivity of exciting the various Xan's at different excitation wavelengths. It is clear from Figure 6 that the Xan absorption spectra strongly overlap with those of Chl (mainly *b*). Therefore, only limited selectivity of Xan excitation can be obtained and always some (at least ~25%) Chl *b* will be excited. In this respect, it is in our opinion strange that in a recent femtosecond pump−probe study of the Xan-to-Chl excitation transfer (*14*) it was claimed that no direct excitation of Chl *b* at 490 nm could be observed. The reconstructed spectrum strongly suggests that at 490 nm Chl *b* contributes about 40% to the absorption spectrum.

In Figures 7 and 8 a comparison is shown between the experimental and simulated ratio between fluorescence excitation and 1−T spectra at room temperature and 40 K, respectively. For the simulated ratio's the 1−T spectrum was calculated from the reconstructed absorption spectrum of Figure 6. The excitation spectra were calculated using the same spectrum, allowing different contributions of the various Xan's, to account for less than 100% Xan-to-Chl excitation transfer efficiency. The ratio's were calculated from 1−T and fluorescence excitation spectra which were normalized on their maximum. We have used the same reconstructed absorption spectrum to simulate the data at 300 and 40 K, which stresses the approximate nature of our simulation. Figure 7 shows the experimental ratio and some simulated ratio's at room temperature. Note for instance that 80% efficiency of either the 494 nm or the 510 nm Xan would lead to a significant dip in the ratio spectrum, above 500 nm which is not observed. We conclude that the singlet energy transfer from these species is rather efficient (>90%). On the other hand the transfer from the 486 nm Xan is rather inefficient (30% ± 20%). The simulations succeed in reproducing a detail like the minimum in the spectrum at about 425 nm. The ratio between the minima at 455 and 485 nm is slightly different in the simulated and experimental spectra. This might be due to differences in the relative Franck−Condon factors (that determine this ratio) of the *in vitro* and *in vivo* Xan absorption spectra. In Figure 8 the same is shown for 40 K. Here the ratio of fluorescence and 1−T deviates more from one (note the different *y*-scale). We estimate from the simulations that the 486 nm Xan hardly transfers excitations to Chl (20% ± 10%) and the efficiencies of transfer from both the 510 and 494 nm Xan's (80% ± 10%) have decreased. Again the minimum at 425 nm is reproduced quite well in the simulations. In Figure 9 a comparison is shown between the same experimental ratio at 40 K and the total simulated ratio for different efficiencies of the transfer from the three Xan's to Chl. Not all features in the experimental ratio are well described by the simulations. The simulations show a higher ratio around 475 nm. This might be due to a small fraction (few percent) of Chl *b* which transfers badly to Chl *a*. Also the shoulder at about 485 nm is more pronounced in the simulations than in the experimental ratio. This might be due to differences in the absorption spectrum of the Xan's in the complex and *in vitro*. The part of the ratio below 470 nm and above 500 nm is described rather well assuming Xan-to-Chl transfer efficien-

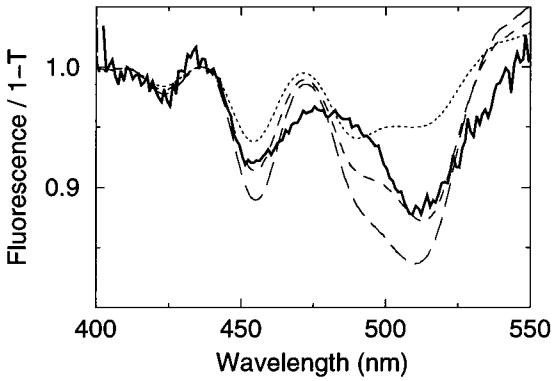

FIGURE 9: Comparison of the experimental (solid line) and simulated (dashed/dotted) ratio of fluorescence excitation and 1−T spectra at 40 K. Simulated ratio's are shown for 90%, 90%, and 30% (dotted), 80%, 80%, and 20% (dashed), and 70%, 70%, and 10% (long dashed) efficiencies of the 510, 494, and 486 nm Xan-to-Chl transfer, respectively

cies of 80% for the 510 and 494 nm Xan's and 20% for the 486 nm Xan.

The observation that at room temperature the total Xan-to-Chl transfer efficiency is about 70% is in conflict with the 100% reported by Siefermann-Harms (*3*) but agrees more with the <80−90% reported by Connelly and co-workers (*14*). We agree with the latter authors that it is extremely important to realize that only part of the absorption in the 450−520 nm region is due to the less efficient transferring Xan's, the major part is due to Chl *b*, which transfers to Chl *a* with close to 100% efficiency.

DISCUSSION

We have shown with the use of low-temperature absorption, T−S, and fluorescence excitation spectroscopy that three spectrally distinct Xan contributions are present in trimeric LHCII with red most absorption peaks at 486, 494, and 510 nm. In the following discussion of these three Xan contributions we assume that our preparations are homogeneous with respect to pigment content, except for Vio, which is not present in all complexes. We also assume that the three to four Xan molecules present in the complex have a distinct absorption spectrum, with their red most maxima at 486, 494, or 510 nm, respectively. This implies that two of Xan's have the same spectrum.

Xan Absorbing at 510 nm. The intensity of the 510 nm shoulder in the absorption spectrum is such that it can only be due to a substoichiometric amount of Xan. If either one Neo or Lut per LHCII trimer would be responsible for the absorption peak at 510 nm, this absorption peak would be significantly more intense. Therefore, we assign this feature to Vio. This assignment is consistent with the observation that upon monomerization most of the Vio is lost. This loss correlates with the disappearance of the 510 nm absorption peak. The reconstruction of the T−S spectrum shows that the same species is responsible for the peak in the T−S spectrum at 525 nm. The small amount of Vio is very efficient in accepting triplets, about 30% of the total amount of triplets formed gives rise to a Vio triplet. An explanation for this could be that almost all LHCII trimers contain one Vio and that this Vio is able to accept triplets from the whole LHCII trimer. The fact that Vio is important for triplet quenching and also shows rather efficient singlet energy transfer indicates that at least one Chl *a* molecule is located close to this Xan and that Vio plays an important photophysical role.

Both subpicosecond pump-probe measurements of Xan-to-Chl singlet transfer (*13*), and microwave selective ADMR measurements (*10*) clearly indicate that the Chl *a* molecule(s) which are in close contact with Vio have an absorption peak at about 670 nm. This correlation between Vio and relatively blue absorbing Chl is further supported by the energy-selective T−S measurements shown in Figure 2.

Xan Absorbing at 494 nm. The T−S measurements on monomers clearly show that the peak in the absorption spectrum at 494 nm is responsible for the maximum in the T−S spectrum at 506 nm. This peak in the absorption spectrum is most likely due to two Xan's. The singlet transfer of these Xan's to Chl is rather efficient (>80%), and these Xan's accept a large fraction of the Chl triplets.

ADMR (*10*) and subpicosecond pump−probe measurements (*13*) have shown that the Chl *a* molecules which are in close contact with this photophysically active, 494 nm Xan molecules, absorb relatively to the red (around 675 nm). Our energy-selective T−S measurements are in agreement with these experiments. It is very likely that these Xan's are the two structurally resolved Xan's (*8*), since they are in close contact with many Chl's. These two Xan's were tentatively assigned to Lut (*8*).

Xan Absorbing at 486 nm. The Xan component with a peak in the absorption spectrum at 486 nm shows hardly any singlet transfer to Chl, nor does it accept a significant amount of triplets from Chl. This inactive Xan should be not too close to Chl's and is most probably not resolved in the crystal structure. Assuming that the two central, active Xan's are Lut this should be Neo. However, we cannot exclude that one of the central Xan's is Neo and one of the Lut's is inactive. We can also not be sure that the Xan content of each LHCII trimer is the same. It is an intriguing observation that this 486 nm Xan seems to be not involved in the photobiophysics of LHCII. We can only speculate about the function of this Xan in LHCII. It might be important for structural stabilization (*6*, *7*) or might be involved in direct quenching of singlet oxygen, like β-carotene in the reaction centre of photosystem II of green plants (*26*). On the other hand it might be possible that triplets are formed on this Xan, but are transferred to the other ones. Such a Car-to-Car triplet transfer has recently been observed in the peridinin−chlorophyll *a* Protein of dinoflagellates (*27*). However, for such a transfer mechanism to be efficient, the Xan's should be in Van der Waals distance. The two Xan's which are structurally resolved in LHCII are much further apart.

ACKNOWLEDGMENT

We thank Wijnand Spierdijk for technical assistance and Dr. Ivo van Stokkum for help with the global analysis of the data.

REFERENCES

1. Van Grondelle, R., Dekker, J. P., Gillbro, T., and Sundström, V. (1994) *Biochim. Biophys Acta 1187*, 1−65.
2. Jansson, S. (1994) *Biochim. Biophys. Acta 1184*, 1−19, and references herein.
3. Siefermann-Harms, D. (1987) *Physiol. Plant. 69*, 561−568.
4. Peterman, E. J. G., Dukker, F. M., van Grondelle, R., and van Amerongen, H. (1995) *Biophys. J. 69*, 2670−2678.

5. Siefermann-Harms, D. (1985) *Biochim. Biophys. Acta 811*, 325−355.
6. Plumley, F. G., and Schmidt, G. W. (1987) *Proc. Natl. Acad. Sci. U.S.A. 84*, 146−150.
7. Paulsen, H., Finkenzeller, B., and Kühlein, N. (1993) *Eur. J. Biochem. 215*, 809−816.
8. Kühlbrandt, W., Wang, N. D., and Fujiyoshi, Y. (1994) *Nature 367*, 614−621.
9. Frank, H. A., and Cogdell, R. J. (1996) *Photochem. Photobiol. 63*, 257−264.
10. Van der Vos, R., Carbonera, D., and Hoff, A. J. (1991) *Appl. Magn. Reson. 2*, 179−202.
11. Carbonera, D., and Giacometti, G. (1992) *Rend. Fis. Acc. Linc. 3*, 361−368.
12. Van der Vos, R., Franken, E. M., and Hoff, A. J. (1994) *Biochim. Biophys. Acta 1188*, 243−250.
13. Peterman, E. J. G., Monshouwer, R., van Stokkum, I. H. M., van Grondelle, R., and van Amerongen, H. (1997) *Chem. Phys. Lett. 264*, 279−284.
14. Connelly, J. P., Müller, M. G., Bassi, R., Croce, R., and Holzwarth, A. R. (1997) *Biochemistry 36*, 281−287.
15. Peterman, E. J. G., Calkoen, F., Gradinaru C., Dukker, F. M., van Grondelle, R., and van Amerongen, H. (1995) in *Photosynthesis: From Light to Biosphere* (Mathis, P., Ed.) Vol. 4, pp 31−34, Kluwer Academic Publishers, Dordrecht.
16. Berthold, D. A., Babcock, G. T., and Yocum, C. F. (1981) *FEBS Lett. 134*, 231−234.
17. Nussberger, S., Dekker, J. P. , Kühlbrandt, W., van Bolhuis, B. M., van Grondelle, R., and van Amerongen, H. (1994) *Biochemistry 33*, 14775−14783.
18. Davies, B. H. (1976) in *Chemistry and Biochemistry of Plant Pigments* (Goodwin, T. W., Ed.) Vol. 2, pp 38−165, Academic Press, London.
19. Lichtentaler, H. K. (1987) in *Plant Cell Membranes* (Packer, L., Ed.) pp 350−382, Academic Press, San Diego, CA.
20. Van Stokkum, I. H. M., Scherer, T., Brouwer, A. M., and Verhoeven, J. W. (1994) *J. Phys. Chem. 98*, 852−866.
21. Bensasson, R. V., Land, E. J., and Truscott, T. G. (1983) *Flash Photolysis and Pulse Radiolysis*, Pergamon Press, New York.
22. Ruban, A. V., Young, A. J., Pascal, A. A., and Horton, P. (1994) *Plant Physiol. 104*, 227−234.
23. Ricci, M., Bradforth, S. E., Jimenez, R., and Fleming, G. R. (1996) *Chem. Phys. Lett. 259*, 381−390.
24. Peterman, E. J. G., Pullerits, T., van Grondelle, R., and van Amerongen, H. (1997) *J. Phys. Chem. B 101*, 4448−4457.
25. Kwa, S. L. S., Völker, S., Tilly, N. T., van Grondelle, R., and Dekker, J. P. (1994) *Photochem. Photobiol. 59*, 219−228.
26. Telfer, A., Dhami, S., Bishop, S. M., Philips, D., and Barber, J. (1994) *Biochemistry 33*, 14469−14474.
27. Carbonera, D., Giacometti, G., and Segre, U. (1996) *J. Chem. Soc., Faraday Trans. 92*, 989−994.

BI9711689